

We are IntechOpen, the world's leading publisher of Open Access books Built by scientists, for scientists

5,800

Open access books available

142,000

International authors and editors

180M

Downloads

Our authors are among the

154

Countries delivered to

TOP 1%

most cited scientists

12.2%

Contributors from top 500 universities



WEB OF SCIENCE™

Selection of our books indexed in the Book Citation Index
in Web of Science™ Core Collection (BKCI)

Interested in publishing with us?
Contact book.department@intechopen.com

Numbers displayed above are based on latest data collected.
For more information visit www.intechopen.com



Deep Learning Algorithms for Efficient Analysis of ECG Signals to Detect Heart Disorders

Sumagna Dey, Rohan Pal and Saptarshi Biswas

Abstract

Electrocardiography (ECG) has been a reliable method for monitoring the proper functioning of the cardiovascular system for decades. Recently, there has been a lot of research focusing on accurately analyzing the heart condition through ECG. In recent days, numerous attempts are being made to analyze these signals using deep learning algorithms, including the implementation of artificial neural networks like convolutional neural networks, recurrent neural networks, and the like. In this context, this chapter intends to present some important techniques for classifying heartbeats based on deep neural networks with 1D CNN. Five ECG signals (N, S, V, F, and Q) standardization are based on the AAMI EC57 standard. The primary focus of this chapter is to discuss the techniques to classify ECG signals in those classes with promising accuracy and draw a clear picture of the current state-of-the-art in this sphere of study.

Keywords: signal processing, electrocardiography, deep learning, 1D convolutional neural network, recurrent neural network

1. Introduction

Cardiac problems are one of the most important problems across the globe. According to autopsy studies, heart disease has increased since the 1960s due to a rise in the frequency of coronary atherosclerosis with resultant coronary heart disease. The number of CVD deaths in India each year is anticipated to increase from 2.26 to 4.77 million between the years 1990 and 2020. The coronary heart disease frequency rates in India have fluctuated from 1.6 to 7.4% in rural populations whereas from 1 to 13.2% in urban populations during the last several decades [1]. Heart disease claims the lives of about 17 lakh individuals in India each year, and the number is estimated to rise to 2.3 crores by 2030. This rise is linked to an increase in smoking and dietary changes, resulting in higher blood cholesterol levels. The symptoms like angina, chest pain, difficulty breathing, edema, fatigue, and lightheadedness may indicate a heart problem or heart attack. Heart attack can lead to cardiac arrest, which occurs when the heart's rhythm is disrupted, or the heart stops beating, and the body can no longer function [2].

Any disorder that affects the cardiovascular system is alluded to as heart disease [3]. Heart disease comes in various forms, each of which affects the heart and blood arteries in distinct ways. The most typical kinds of heart disease are coronary artery disease, arrhythmia, heart valve disease, and heart failure [4]. Coronary artery disease is the most noticeable type of heart disease. It happens when plaque accumulates in the arteries that deliver blood to the heart. It can cause a reduction in blood flow to your heart muscle, preventing it from receiving the oxygen it requires. Atherosclerosis, often known as artery hardening, is the most common cause of the illness. Arrhythmia refers to an improper beating of the heart [5]. It happens when the electrical impulses that regulate the heartbeat do not even function properly. As a result, the heart may beat excessively fast, too slowly, or in an irregular pattern. Heart valve disease occurs when a heart valve is damaged [6]. Infectious diseases such as rheumatic fever, congenital heart disease, excessive blood pressure, coronary artery disease are all causes of heart valve disorders. Heart failure does not imply that the heart has ceased to beat. A condition in which the heart is not pumping blood as efficiently as it should be to satisfy the body's demands. There are some more heart diseases like pericardial disease, myocardial infarction [7], cardiomyopathy, mitral valve regurgitation, congenital heart disease, etc.

Over the last several decades, the rapid advancement of cardiology has profoundly changed the natural course of cardiac patients. Cardiac care has evolved, with technology playing an increasingly significant role. With the appropriate technology and artificial intelligence (AI) and machine learning, cardiac care providers have been motivated to improve treatment methods [8]. Then there's remote care that enables electrocardiogram (ECG) diagnosis [9], which uses cloud technology and Bluetooth-enabled cardiac devices to test the parameters and send them back to healthcare practitioners without attending the clinic. Some emerging technologies used every day in cardiology are transcatheter mitral and tricuspid valve interventions, artificial intelligence, wearable devices, big data, structured reporting, robots in the cath lab, virtual and augmented reality, FFR technologies, holographic procedural navigation in the Cath Lab, etc. [10].

There are many cardiac implantable electronic devices like pacemakers, implanted cardioverter defibrillators (ICDs), biventricular pacemakers, and cardiac loop recorders, which are used to control or monitor irregular heartbeats in persons with specific heart rhythm problems and heart failure. An implanted cardioverter-defibrillator is a device that can do cardioversion, defibrillation, and cardiac pacing. ICD is capable of rectifying the majority of life-threatening cardiac arrhythmias. A pacemaker is a device that is implanted beneath the skin and communicates with the heart through electrical leads. Pacemakers are used to treat bradycardia, a condition where the heart beats too slowly (less than 60 times per minute). The pacemaker sends electrical pulses to the heart to maintain it beating normally. A biventricular pacemaker is a compact, battery-operated device and light. This gadget aids with the proper pumping of your heart. It also protects from harmful cardiac arrhythmias. An implantable loop recorder is a heart-monitoring device implanted beneath the chest skin. It has a variety of applications. Searching for reasons of fainting, palpitations, very rapid or slow heartbeats, and hidden rhythms that might cause strokes are among the most prevalent. Computer-aided diagnosis (CAD) [11] refers to software that helps clinicians understand medical images. The radiologist or other medical expert must assess and evaluate a large amount of data in a short amount of time using imaging modalities such as X-ray, MRI, and ultrasound diagnostics. The Kurt Rossmann Laboratories for Radiologic Image Research in the Department of

Radiology at the University of Chicago began large-scale systematic research and development of several CAD methods in the early 1980s. The idea of computer-aided design was established in 1966 and has been completely implemented since 1980.

Nowadays, computer-aided diagnosis has become a contentious research topic in medical imaging and diagnostic radiology research. CAD technology aids in the improvement of the performance of radiologists in increasing productivity by cost-effectively enhancing sensitivity rate. CAD can improve image diagnostic accuracy by detecting illnesses that are too premature to be detected by naked eyes. It enables early detection, which can lead to better treatment results. Computer-aided detection is a relatively new advancement in the area of breast imaging that aims to increase the throughput of radiologists to identify diseases like breast cancer [12] even at an early stage. In recent times, computer-aided diagnosis is used to diagnose acute lymphoblastic leukemia, which suggested a solution to the flaws in manual diagnosis techniques. Even ECG-based computer-aided diagnosis [13] is also used for cardiovascular diseases which have the potential to improve diagnosis accuracy while also lowering costs.

Medical images nowadays play a crucial role in the identification and diagnosis of a wide range of disorders. To aid in the interpretation of medical images, a variety of computer-aided detection and diagnosis technologies have recently been developed in order to achieve a more reliable and accurate diagnosis. CT, MR imaging, digital radiography, biomagnetism, and optical range sensing are examples of imaging systems that take advantage of sophisticated computer technology.

The real-life problem with manual experimentation is that manual diagnostic procedures are time-consuming, less accurate, and prone to mistakes due to different human variables such as stress, exhaustion, fatigue, and so forth. As a result, many automated techniques have been developed to combat the flaws in manual diagnostic approaches. When compared to manual diagnosis procedures, these computer-aided technologies are faster, more dependable, more efficient, more standardization and more accurate. Computer-aided diagnosis (CAD) aids in the calculation of computational and statistical features that people cannot gather visually or intuitively. Computer-assisted diagnosis also reduces the reliance on the operator in ultrasonic imaging and makes the diagnosis procedure reproducible. Interference testing and 3D animations are simple to accomplish in computer-aided diagnosis [14].

Machine learning has been applied in a variety of fields all over the world and the health industry is no exception. On the other hand, deep learning is part of the family of machine learning algorithms relying on representation and artificial neural networks are being utilized for the analysis of medical data. For quite some time, these algorithms were used to assess patients' status with respect to the image or non-image-based medical data acquired using new generation medical equipment. These developments are attributable to the emergence of new CAD systems known as knowledge-based systems, including expertise or knowledge. As a result, the modern CAD systems include some intelligence [15]. The major job of the software related to these systems nowadays is to automate the analytical phases. To ensure that components and assemblies achieve design standards, CAD software is used to make computer modeling, fit them together, and simulate their performance. Because design reviews, conducted by specialists, evaluate if changes should be made, the analytical phases of the design process are repeated (design synthesis). Design synthesis may be done immediately with AI-based technologies without the need for a separate design review, and they are correctly implemented.

Based on the recent advancements, computer-aided diagnosis is used to diagnose heart abnormalities such as arrhythmias and heart blockages using electrocardiogram (ECG) signal analysis [16]. Although electrocardiography (ECG) is affordable and commonly available, ECG abnormalities are not specific for the diagnosis of congestive heart failure (CHF) which is the inability of the heart to efficiently circulate blood throughout the body without a rise in intracardiac pressure. Based on the ECG, a well-designed computer-aided detection (CAD) system for CHF might possibly eliminate subjectivity and give a quantitative evaluation for better decision-making.

Cardiologists and medical practitioners frequently utilize ECG to assess heart health. The difficulty in identifying and classifying distinct waveforms and morphologies in ECG signals is the major issue with manual analysis. This task is both time-consuming and error-prone for a human. Cardiovascular illnesses are the leading cause of mortality worldwide, accounting for around one-third of all fatalities. Millions of individuals, for example, suffer from irregular heartbeats, which can be fatal in some circumstances. As a result, precise and low-cost arrhythmic heartbeat diagnosis is extremely desirable.

Many research in the literature investigated the utilization of machine learning approaches to reliably detect abnormalities in ECG data to solve the drawbacks present in human analysis. Pre-processing, like passing through bandpass or high pass filter, is used in most of these methods to prepare the signal to be compatible for machine-based analysis. The handcrafted features, which are typically statistical summarizations of signal windows, are then retrieved from these signals and employed in subsequent processing. For the last categorization task, conduct an analysis.

In terms of the conclusion, for ECG, traditional machine learning algorithms [2] like support vector machines, multi-layer perceptrons, decision trees, and other methods of analysis were used previously. Automated feature extraction and representation approaches have been shown to be more scalable and capable of producing more accurate predictions, according to current machine learning research. In this study, we are going to elaborate on a few of the new emerging and compatible technologies and their applications.

The rest of the article has been organized in the following manner. First, Section 2 provides a brief theoretical and mathematical background related to this domain of study which is followed by the problem statement in Section 3. Next, Section 4 discusses about the significance of noise removal with stages of data processing. Section 5 gives a brief survey about the recent state-of-the-art techniques related to automated signal processing of ECG signals that is followed by the promising experimental results reported in the recent literature. Finally, Section 7 concludes this chapter.

2. Theoretical and mathematical background

2.1 Mathematical foundation

In signal processing [17], several mathematical methods like sampling frequency, Nyquist filtering, Fourier analysis series and transform, Z transform, pole zero plot are used for processing signals.

The reduction of a continuous-time signal to a discrete-time signal is known as sampling and the sampling frequency represents the number of samples per second collected from a continuous signal to create a discrete or digital signal. There are few applications of the sampling process. The sampling process is utilized in music

recordings to ensure sound quality. The sampling technique is also used to convert analog to discrete data. It is also used in speech recognition systems, radar and radio navigation, sensor data evaluation, modulation and demodulation, and pattern recognition systems.

2.1.1 Sampling frequency or sampling rate

The sampling frequency [18] or sampling rate f_s is defined as the average number of samples acquired in 1 second, therefore $f_s = \frac{1}{T}$ where T is the sampling period and is measured with the unit samples per second or hertz. The sampling theorem indicates the lowest sampling frequency where a continuous-time signal must have been uniformly sampled in order for the original signal to be fully recovered or reconstructed using just these samples.

If a continuous-time signal has no frequency components greater than a sampling rate of W Hz (where W is called the bandwidth), then uniform samples taken at a rate of f_s samples per second can be used to identify it completely [19]. This implies $f_s > = 2W$ and when it comes to the sampling period $T < = \frac{1}{2W}$. Here $2W$ is termed as the Nyquist rate.

2.1.2 Nyquist filter

A Nyquist filter is an electrical filter that equalizes the visual characteristics of TV receivers. In receivers, a Nyquist filter is utilized to equalize the low and high-frequency components of the VF signal. It plays an essential role in the creation of n bandlimited pulses in wired and wireless communication systems to ensure minimal inter symbol interference. Its principal application is as a pulse-shaping filter. Nyquist filters are a form of multi-rate finite impulse response filter that is also known as M^{th} band filters.

The following equation indicates the impulse response of a Nyquist filter $h(n)$:

$$h(Mn + k) = \begin{cases} c & n = 0 \\ 0 & otherwise \end{cases} \quad (1)$$

where, c and k are constants.

The following equation satisfies the z -transform of a Nyquist filter $H(z)$:

$$\sum_{k=0}^{M-1} H(zW^k) = Mc = 1 \quad (2)$$

where, $W = e^{-\frac{j2\pi}{M}}$ and $c = \frac{1}{M}$.

The frequency responses of all M uniformly shifted versions of $H(z)$ add up to a constant because the frequency response of $H(zW^k)$ is the shifted version of the frequency response of $H(z)$.

2.1.3 Fourier series and Fourier transform

The Fourier series is a periodic function made up of harmonically compatible sinusoids that are integrated together using a weighted summation. The Fourier series is an infinite series that can be used to solve several forms of differential equations. It's

mainly composed of an infinite sum of sines and cosines, and it's valuable for evaluating periodic functions since it's periodic. The Fourier series is widely utilized in telecommunications systems for voice signal modulation and demodulation.

The Fourier transform is a technique for transforming time-domain signals to frequency-domain signals. The Fourier transform is a useful image processing method for decomposing an image into sine and cosine components. The image in the Fourier or frequency domain is represented by the output of the transformation, whereas the spatial domain equivalent is represented by the input image. It's utilized in electrical circuit design, solving differential equations, signal processing, signal analysis, image processing, and filtering, among other things.

The Fourier transform is a mathematical approach for converting a time function, $x(t)$, to a frequency function, $X(\omega)$. It has a lot in common with the Fourier series. The Fourier transform of a function can be determined as a specific instance of the Fourier series when the period is $T \rightarrow \infty$.

The Fourier transform of a sequence is represented as:

$$x(t) = \sum_{n=-\infty}^{\infty} c_n e^{jn\omega_0 t} \quad (3)$$

where c_n is provided by the Fourier series analysis equation:

$$c_n = \frac{1}{T} \int_T x(t) e^{-jn\omega_0 t} dt \quad (4)$$

It can also be written as:

$$X(e^{j\omega}) = \sum_{n=-\infty}^{\infty} [n] e^{-j\omega n} \quad (5)$$

As $T \rightarrow \infty$ the initial frequency, $\omega_0 = \frac{2\pi}{T}$ decreases dramatically and the quantity $n\omega_0$ becomes a continuous quantity that may take on any value (because n has a range of $\pm\infty$). So, we generate a special variable $\omega = n\omega_0$ and set $X(\omega) = Tc_n$. The analytical equation for the Fourier transform is obtained by substituting these values in the previous equation. This transform is also called the forward Fourier transform.

The analysis equation of forward Fourier transform is:

$$X(\omega) = \int_{-\infty}^{+\infty} X(t) e^{-j\omega t} dt \quad (6)$$

On the other hand, the synthesis equation of inverse Fourier transform is:

$$x(t) = \frac{1}{2\pi} \int_{-\infty}^{+\infty} X(\omega) e^{j\omega t} d\omega \quad (7)$$

2.1.4 Z-transform

Z transform is a useful mathematical tool for converting differential equations to algebraic equations. Z transform is utilized when converting a discrete-time domain signal to a discrete frequency domain signal. It has a broad range of statistical and digital signal processing applications. It is mostly used to process and evaluate digital data.

The bilateral z-transform of a discrete-time signal $x(n)$ is given as:

$$Z.T[x(n)] = X(Z) = \sum_{n=-\infty}^{\infty} x(n)z^{-n} \quad (8)$$

The unilateral z -transform of a discrete-time signal $x(n)$ is represented by the following equation:

$$Z.T[x(n)] = X(Z) = \sum_{n=0}^{\infty} x(n)z^{-n} \quad (9)$$

Fourier transform and Z transform equations have an operation in an embedded system. If we substitute z with $e^{j\omega}$ then the z -transform becomes the Fourier transform. On the other hand, when $|z| = 1$, the Fourier transform is simply $X(z)$ with $z = e^{j\omega}$ and the z -transform correlates to the Fourier transform. If we express z in polar form, we get $z = re^{j\omega}$.

A system's Fourier transform and z -transform can be written as:

$$H(\omega) = \sum_{k=0}^M b_k e^{-j\omega k} \quad (10)$$

$$H(z) = \sum_{k=0}^M b_k z^{-k} \quad (11)$$

$$H(\omega) = H(e^{j\omega}) = H(z) \Big|_{z=e^{j\omega}} \quad (12)$$

2.1.5 Pole-zero plot

The pole-zero plot is a valuable tool for relating a system's Frequency domain and Z -domain representations. A pole-zero plot is a graphical depiction of a rational transfer function in the complex plane that aids in the communication of system attributes.

Pole-zero plot can be expressed as the following equation:

$$H(z) = \frac{B(z)}{A(z)} = \frac{\sum_{k=0}^M b_k z^{-k}}{1 + \sum_{k=0}^N a_k z^{-k}} \quad (13)$$

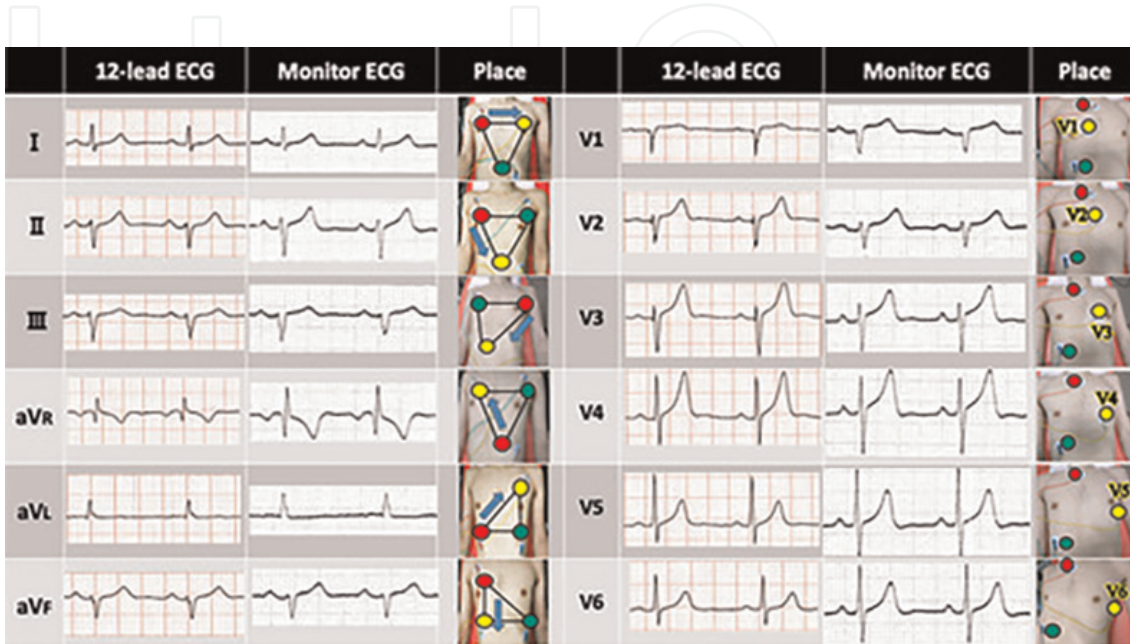
where the numerator and denominator are both polynomials in z . The zeros of $H(z)$ are the values of z for which $H(z) = 0$, while the poles of $H(z)$ are the values of z for which $H(z)$ is ∞ . M and N are the order of the numerator and denominator polynomial, respectively. On the other hand, b_k is the m^{th} coefficient of the numerator polynomial whereas a_k is the n^{th} coefficient of the denominator polynomial.

2.2 ECG signal

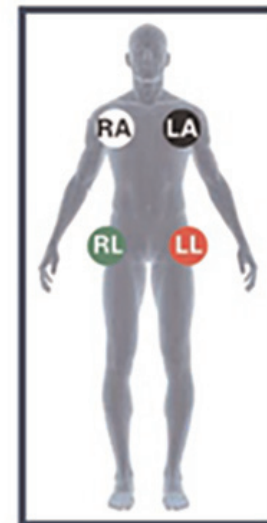
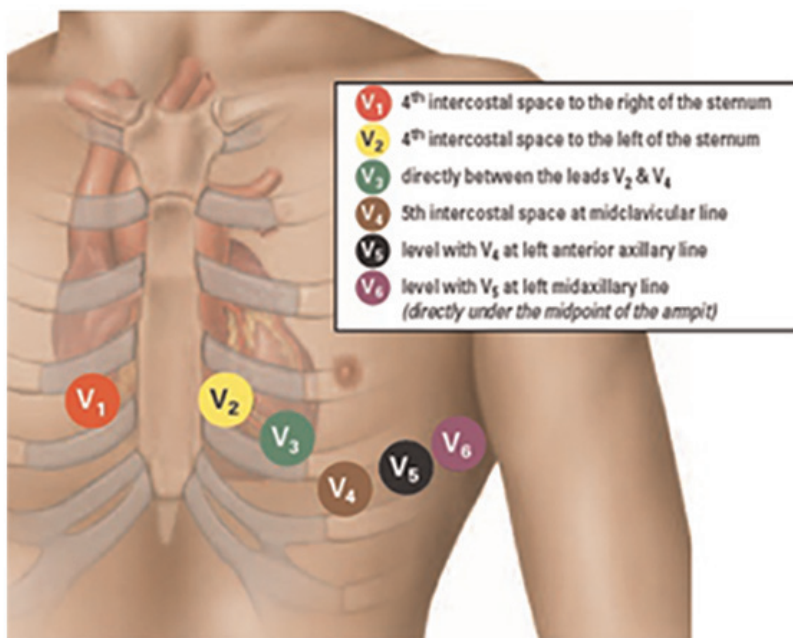
The electrocardiogram (ECG) signal is a representation of the electrical impulses of the heart that can be seen from the strategic points of the human body. It can be visually depicted by a quasi-periodic voltage signal. ECG refers to a 12-lead ECG recorded while laying down and electrodes or sticky patches are put on the body surface and often over the chest and limbs to record a standard surface ECG. These electrode wires are linked

to a 12-lead ECG machine which records data from 12 distinct locations on the body's surface. The aggregate amplitude of the heart's electrical potential is then monitored and recorded over a period of time from those distinct angles ("leads").

The graphical representation of the heart's electrical activity is formed by analyzing numerous electrodes in **Figure 1(a)**. There are three types of leads: limb augmented limb, and precordial or chest. Three limb leads and three augmented



(a)



- RA Right Arm
- LA Left Arm
- LL Left Leg
- RL Right Leg

(b)

Figure 1. 12 leads ECG. a) Signals from 12 Leads ECG [20]. b) Position of placements of the 12 leads on human body [21].

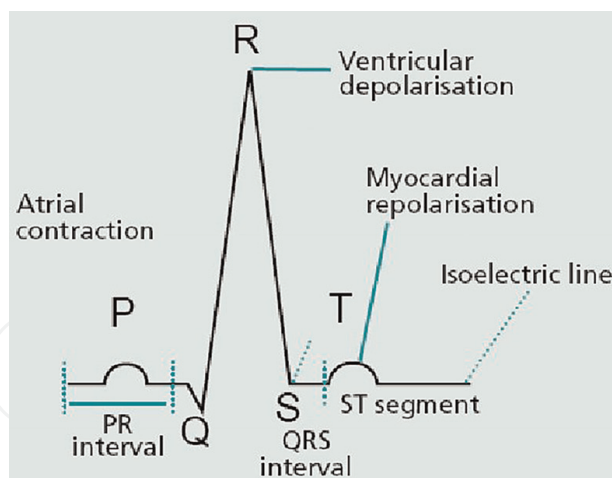


Figure 2.
PQRST waveform [22].

limb leads are organized in the coronal plane like the spokes of a wheel, and six precordial leads or chest leads are organized in the perpendicular transverse plane. In three-dimensional space, each of the 12 ECG leads represents a distinct direction of cardiac activation. The conventional ECG leads are denoted as lead I, II, III, aVF, aVR, aVL, V1, V2, V3, V4, V5, and V6. The limb leads are I, II, III, aVR, aVL, and aVF whereas the precordial leads are V1, V2, V3, V4, V5, and V6.

The 12-lead ECG is typically made up of 10 electrodes linked to the body, each monitoring a distinct electrical potential difference. The 10 electrodes in a 12-lead ECG are RA, RL, LA, LL, V1, V2, V3, V4, V5, and V6. Each of the 10 electrodes has a different placement as shown in **Figure 1(b)**. RA is used to place on the right arm and similarly, LA is used to place on the left arm. RL is located in the lower end of the inner portion of the calf muscle on the right leg, similarly, LL is placed in the same standard position but on the left leg. V1 is placed in the fourth intercostal space (between ribs 4 and 5) immediate right of the sternum. V2 is placed in the fourth intercostal space (between ribs 4 and 5) immediate left of the sternum. V3 is placed between leads V2 and V4 where V4 is placed in the fifth intercostal space (between ribs 5 and 6) in the midclavicular line. On the other hand, V5 and V6 are placed in the left anterior axillary line and midaxillary line, respectively. The electrodes which are located on the limbs are called limb leads which are leads I, II, and III. Lead I refer to the voltage difference between LA and RA, that is, $\text{Lead I} = \text{LA} - \text{RA}$. Similarly, Lead II denotes the voltage difference between LL and RA, that is, $\text{Lead II} = \text{LL} - \text{RA}$. And Lead III denotes the voltage between LL and LA, that is, $\text{Lead III} = \text{LL} - \text{LA}$.

Lastly, a PQRST complex is part of an ECG complex which is shown in **Figure 2**. The P wave is produced by the sinoatrial node which is the heart's pacemaker and implies atrial depolarization in an ECG complex. The atrioventricular node generates the QRS wave. Ventricular depolarization is represented by the QRS, while ventricular repolarization is indicated by the T wave.

2.3 Deep learning

2.3.1 Artificial neural network

In biology, neural networks develop the structure of animal brains, where the phrase "artificial neural networks" comes from. It is widely used in deep learning

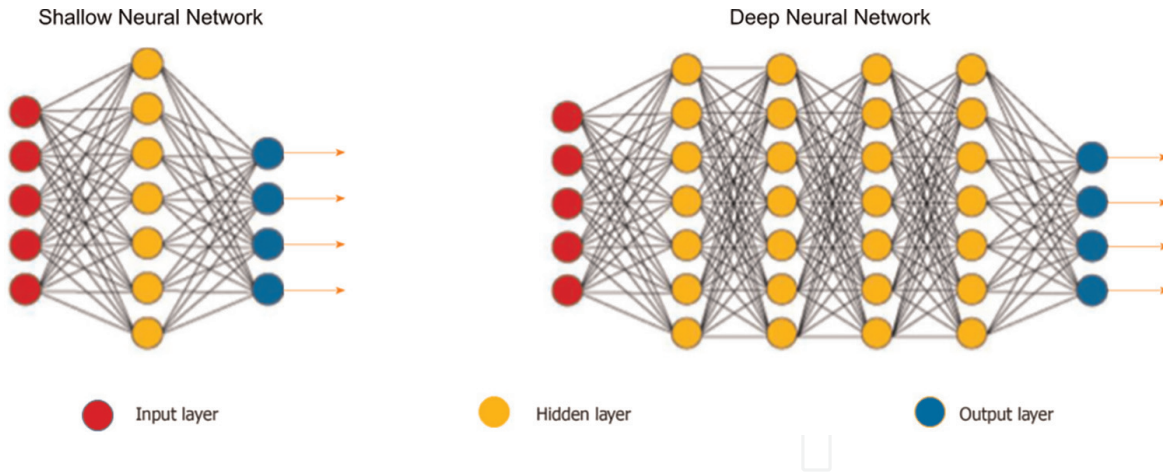


Figure 3.
Architecture of a general ANN [24].

algorithms. An artificial neural network (ANN) [23] generally consists of three layers, namely, the input layer, hidden layer, and output layer. The hidden layers are present in-between input and output layers. It executes all the calculations to find hidden features and patterns. A shallow neural network consists of only one hidden layer and a deep neural network consists of multiple hidden layers. Generally, each node in one layer is linked to every other node in the next layer. By increasing the number of hidden layers, the network becomes deeper. This architecture is demonstrated in **Figure 3**.

2.3.2 Convolutional neural network

Based on the concept of ANNs, a convolutional neural network (CNN) [25] was formulated which is a deep learning method that can take an image as input and learn some filters that can be used to extract essential features from those images. The brain is the source of inspiration for convolutional neural networks. CNN performs a linear mathematical procedure known as a convolution in the several hidden layers between an input and output layer. The general mathematical expression of convolution operation is provided in the following equation:

$$Y = W * X + b \quad (14)$$

where W and X represent the filter and the input, respectively whereas b represents the bias matrix and the $*$ represents the convolution operation between the matrices W and X .

CNN's have the benefit of being able to construct an internal demonstration of a two-dimensional image. This enables the model to learn position and scale in different data formats, which is essential when working with images.

2.3.3 Recurrent neural network

A recurrent neural network (RNN) [26] is a form of artificial neural network which is designed to operate with time series, analyzing temporal and sequential data. It's one of the algorithms responsible for the incredible advances in deep learning over the last few years. RNN can handle inputs/outputs of varying lengths. The idea of

“memory” in RNNs is used to store the states or information of earlier inputs in order to generate the sequence’s next output. It has the ability to store or memorize historical information.

Long short term memory (LSTM) [27] is a type of recurrent neural network and LSTM networks are well-suited to categorize, processing, and generating predictions based on time series data as there might be delays of undetermined duration between critical occurrences in a time series. LSTMs were designed to explode gradients and solve the problem of vanishing gradients that can occur while training standard RNNs.

LSTM uses the concept of gates. It has three gates which are input gate, forget gate, and output gate. The input gate determines what new information will be stored in the cell state. The forget gate determines what information to throw away from the cell state whereas the output gate is used to activate the LSTM block’s final output. In LSTM, output of the gates are operated with sigmoid activation functions, which calculates a value between 0 and 1, which is usually rounded to either 0 or 1 depending upon a predetermined threshold. “0” indicates that the gates are blocking everything and “1” denotes gates that enable everything to pass through it. The LSTM gates have the following equations:

$$\begin{aligned} i_t &= \sigma(w_i[h_{t-1}, x_t] + b_i) \\ f_t &= \sigma(w_f[h_{t-1}, x_t] + b_f) \\ o_t &= \sigma(w_o[h_{t-1}, x_t] + b_o) \end{aligned} \quad (15)$$

where, i_t, f_t, o_t represents input, forget, and output gates, respectively whereas w_x, b_x and x_t represents weights and biases of gate x and input at the current timestamp, respectively. On the other hand, σ is the sigmoid function. Lastly, h_{t-1} indicates the output of the LSTM block at $t - 1^{th}$ timestamp.

The cell state, candidate cell state, and final output equations are given as follows:

$$\begin{aligned} \bar{c} &= \tanh(w_c[h_{t-1}, x_t] + b_c) \\ c_t &= f_t * c_{t-1} + i_t * \bar{c}_t \\ h_t &= o_t * \tanh(c^t) \end{aligned} \quad (16)$$

where, c_t and \bar{c}_t represents cell state and candidate for cell state at timestamp(t) where the rest of the notations follows from the previous equations.

The architecture of LSTM at any timestamp t is shown in **Figure 4**.

Bidirectional LSTMs [29] are a kind of LSTM that can be used to increase model performance on sequence classification issues. Bidirectional long-short term memory is the process of allowing any neural network to store sequence information in both backward (future to past) and forward (forward to future) directions. BI-LSTM is typically used when sequence to sequence activities are required. Text classification, speech recognition, and forecasting models can all benefit from using this type of network. **Figure 5** shows the architecture of a BI-LSTM.

3. Problem statement

Before the invention of CAD, diagnosis used to be done manually and manual diagnostic procedures were time-consuming, less accurate. In the manual diagnostic

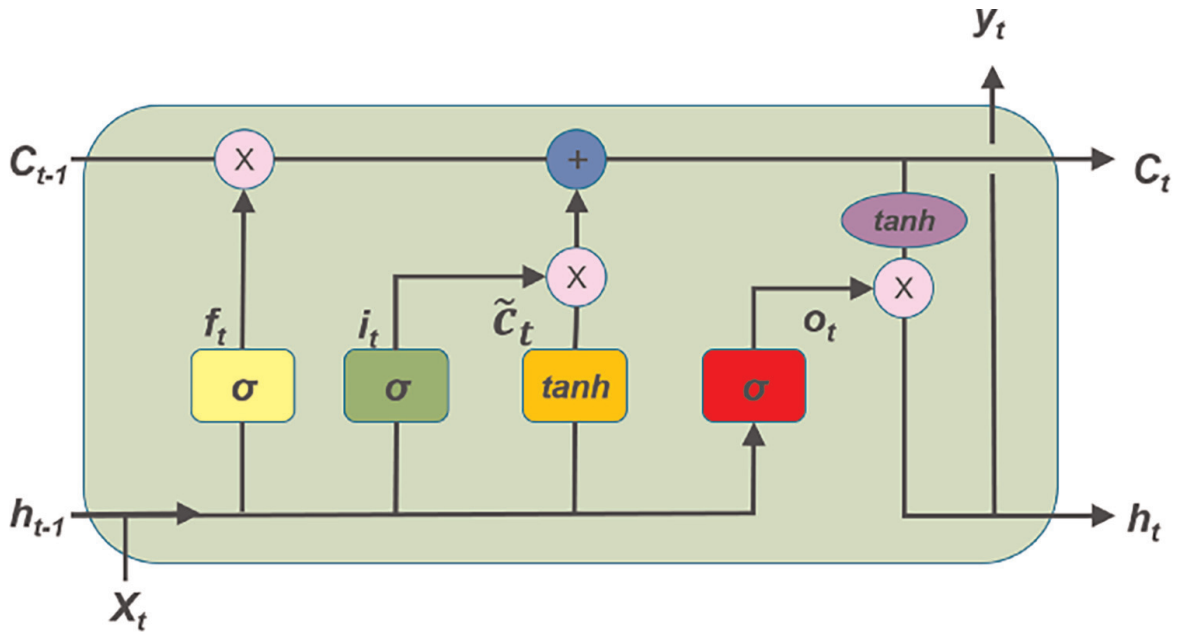


Figure 4.
Graphical representation of LSTM unit [28].

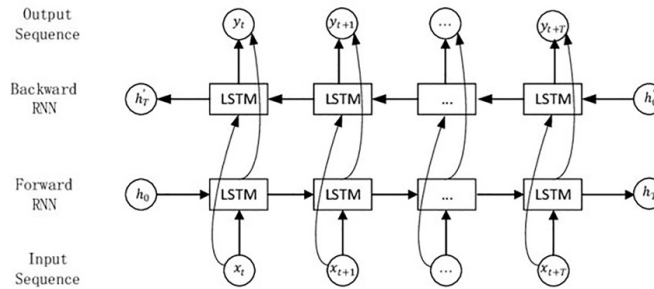


Figure 5.
Graphical representation of bi-directional LSTM unit [30].

procedures, there might be errors in the calculation of computational and statistical features. To counteract the faults in manual diagnostic procedures, deep learning has been introduced to diagnosis. CAD application has heightened the diagnostic performance of non-expert radiologists. Regardless of radiologist expertise, the fundamental benefit of CAD is the minimum false-negative rate and enhanced sensitivity. CAD technologies are faster, more dependable, more accurate and also help to improve in the calculation of computational and statistical features [31]. In this regard, this study focuses on speculating about some of the valuable technologies and trying to approach a conventional solution.

4. Effect of noise in ECG signals and importance of data preprocessing

Noise is an undesirable signal which disrupts the original message signal and causes the message signal's parameters to be altered. Noise distorts the message and hinders it from being understood in an intended manner. When there is loud,

distracting noise that disrupts the communication assimilation process, comprehension suffers.

There is no signal without noise. The signal strength may be affected or aided by noise. Noise can cause signal distortion, which is most noticeable in agitated receivers. Both analog and digital systems suffer from noise, which diminishes their performance. Noise degrades the quality of the received signal in analog systems. Noise reduces the overall performance of a digital system because it necessitates retransmission of data packets or additional coding to recover data in the event of an error. The most prevalent and evident issue produced by signal noise is the distortion of the processed signal, which causes inaccurate interpretation or display of a process state by the equipment. Unusual signal noise can cause an apparent signal loss. Noise filtering is incorporated into most current electrical devices. However, in excessively loud circumstances, this filter may not be sufficient, resulting in the device getting no signal and no connection.

The presence of noise can make it difficult or impossible to identify a representative ECG signal. Noises in the ECG signal can lead to incorrect interpretation. In the ECG signal, there are primarily two kinds of noise. Electromyogram noise, additive white Gaussian noise, and power line interference are examples of high-frequency noises. Power line interference distorts the amplitude, duration, and shape of low-amplitude local waves of the ECG signal. Baseline wandering is an example of low-frequency noise. Baseline wandering alters the ECG signal's ST-segment and LF components.

Noise can be reduced by keeping the signal wires as short as possible or by keeping the wires away from electrical machinery. By using differential inputs, noise can be reduced from both wires. Noise also can be reduced by filtering the signal or by using an integrating A-D converter to reduce mains frequency interference.

There are various ECG denoising techniques [32] that are being used to reduce the noise from signals. Some ECG denoising techniques are EMD-based models, deep-learning-based models, wavelet-based models, sparsity-based models, Bayesian-filter-based models, hybrid models, discrete wavelet transform, etc.

The discrete wavelet transform is a digital processing computational technique that allows for electrical noise with a higher signal-to-noise ratio than lock-in amplifier equipment. A discrete wavelet transform decomposes a signal into a number of sets, each set including a time series of coefficients that describe the signal's time evolution in the associated frequency band.

The process of converting raw data into a comprehensible format is known as data preprocessing. Dealing with raw data is not suitable, thus this is a key stage in data mining. Before using machine learning or data mining methods, make sure the data is of high quality. In every brain-computer interface-based application, preprocessing data is a necessary and significant step. It checks the accuracy, completeness, believability, consistency, interpretability, timeliness of the data. It assists with the removal of undesirable artifacts from the data and prepares it for subsequent processing.

5. State-of-the-art techniques

Peimankar et al. [33] proposed a deep learning model for real-time segmentation of heartbeats which might be utilized in real-time telehealth diagnostic systems. The

proposed technique integrates a CNN and an LSTM model to predict and analyze the onset, peak, and offset of various heartbeat waveforms such as the P-wave, QRS complex, T-wave, and no wave. The proposed model is also known as DENS-ECG model. Using 5-fold cross-validation, this model is trained and evaluated on a dataset of 105 ECGs with a length of 15 min each. It attains an average sensitivity and accuracy of 97.95 and 95.68%, respectively. In addition, the method is calibrated on an unknown dataset to assess how robust it is at detecting QRS with a sensitivity of 99.61% and accuracy of 99.52%. This model illustrates the combined CNN-LSTM model’s adaptability and accuracy in delineating ECG signals. The accuracy of the proposed DENS-ECG model in recognizing ECG waveforms leaves the door open for cardiologists to apply this algorithm in-house to evaluate ECG recordings and diagnose cardiac arrhythmias. This model is provided in **Figure 6**.

In **Figure 6**, noise reduction refers to the filtering of the ECG signals to reduce noise and remove baseline wanders. In the segmentation, the ECG signals are divided into 1000-sample chunks and sent into the model as input. Then the segmented ECG signals are split into two sets to separate the testing set from a non-testing set. This model used a 5-fold cross-validation technique to provide a more trustworthy performance in terms of interpretability. The model consists of eight layers, including an input layer, three 1D convolution layers, two BiLSTM layers, and a dropout layer. And the Adam optimization algorithm is used to validate the algorithm, which is radically different from the steepest gradient descent (SGD) optimization technique and achieved higher performance on the validation. The trained model is tested on 26 unseen test records from the QTDB dataset to assess the classifier’s performance. Furthermore, the model is evaluated for QRS detection on the unexplored MITDB dataset.

Jambukia et al. [34] represented an overview of ECG classification into arrhythmia categories and stated that classification of electrocardiogram (ECG) signals plays a crucial role in the monitoring heart diseases as early and precise diagnosis of arrhythmia types is essential for monitoring cardiac disorders and selecting the best treatment option for a patient. The survey outlines the challenges of ECG classification and provides a comprehensive overview of preprocessing approaches, ECG databases, feature extraction techniques, ANN-based classifiers, and performance measures for

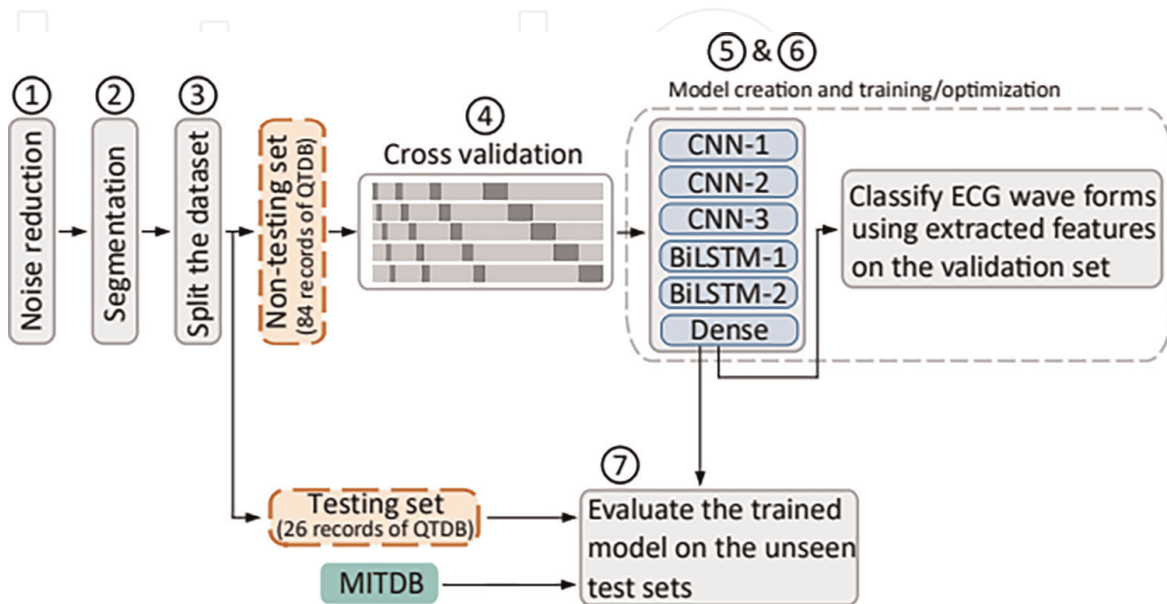


Figure 6. Flowchart of the proposed DENS-ECG model [33].

evaluating the classifiers' accuracy. According to the survey, many researchers have worked on ECG signal classification. They have used different pre-processing techniques, various feature extraction techniques, and classifiers. For ECG categorization, the majority of the researchers used the MIT-BIH arrhythmia database. A. Dallali et al. used DWT to extract the RR interval and then used Z score to normalize it. They classified ECG beats using FCM. They achieved a 99.05% accuracy rate. RR interval and R point position are two characteristics retrieved using DWT. FCM was used for pre-classification, while 3-layer MLPNN was used for final classification. They were able to reach a 99.99% accuracy rate.

Saadatnejad et al. [35] proposed an ECG classification model, which was suggested for continuous cardiac detection on wearable devices with limited processing resources. This model is demonstrated in **Figure 7** in detail. The model works in such a way that the incoming computerized ECG data were first split into heartbeats and their RR interval while wavelet characteristics were extracted. The ECG signal as well as the extracted characteristics were then put into two RNN-based models that categorized every heartbeat. After that, the two outputs were combined to create the final categorization for every pulse. The suggested method fits the temporal criteria for continuous and real-time execution on wearable devices. Unlike many compute-intensive deep-learning-based techniques, the proposed methodology is accurate and lightweight, allowing wearable devices to have continuous monitoring with accurate LSTM-based ECG categorization having negligible computing expenses while running indefinitely on wearable devices with modest processing capability.

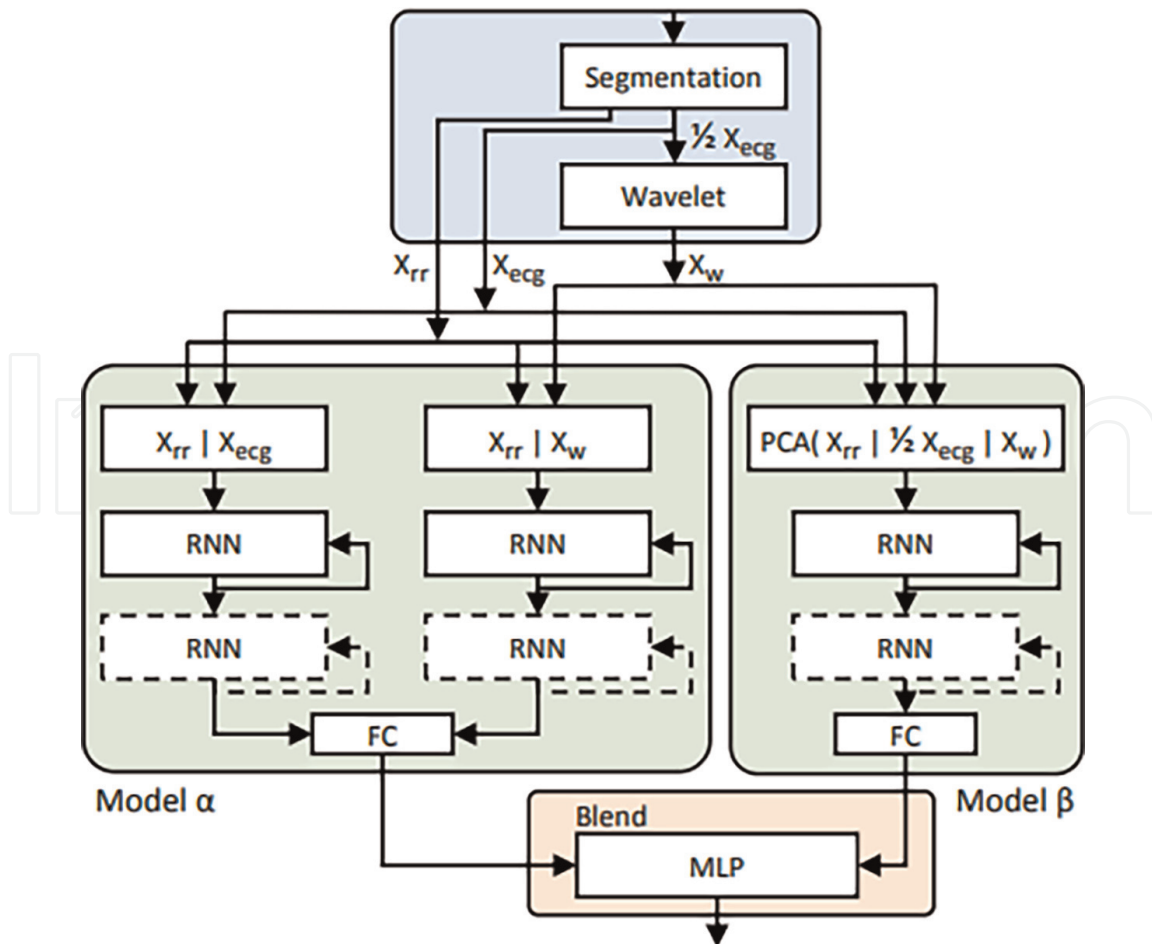


Figure 7.
 The proposed algorithm of LSTM-based ECG classification model [35].

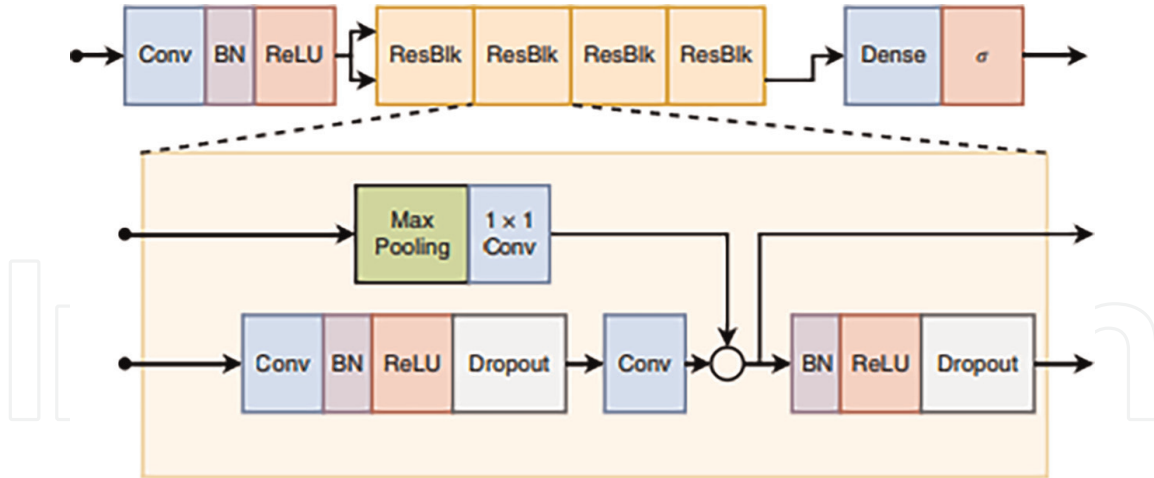


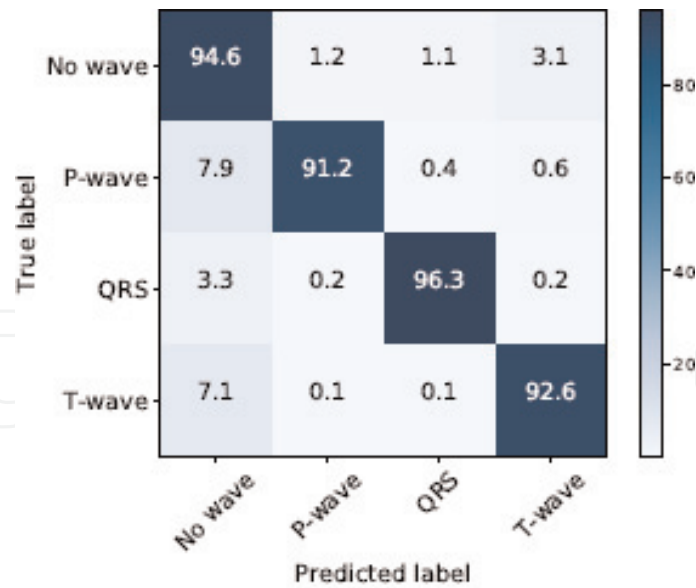
Figure 8.
The DNN architecture used for ECG classification [36].

Ribeiro et al. [36] had proposed an end-to-end DNN competent of accurately identifying six ECG abnormalities in S12L-ECG examinations, with diagnostic performance comparable to that of medical residents and students. This DNN model trained on data from the Clinical Outcomes in Digital Electrocardiology research which included over 2 million labeled tests analyzed by the Telehealth Network of Minas Gerais. The DNN surpassed cardiology resident medical practitioners in detecting six different types of abnormalities in 12-lead ECG recordings with F1 scores over 80% and specificity exceeding 95%. These results suggest that DNN-based ECG analysis, which was previously tested in a single-lead scenario, generalizes well to 12-lead examinations, bringing the technology closer to practical use. This model has the potential to lead to more accurate automated diagnosis and better clinical practice. Even professional assessment of complex and borderline cases appears to be essential in this future scenario, the implementation of such automatic interpretation by a DNN algorithm may increase the population's access to this fundamental and valuable diagnostic test. **Figure 8** shows the deep learning model used in this work.

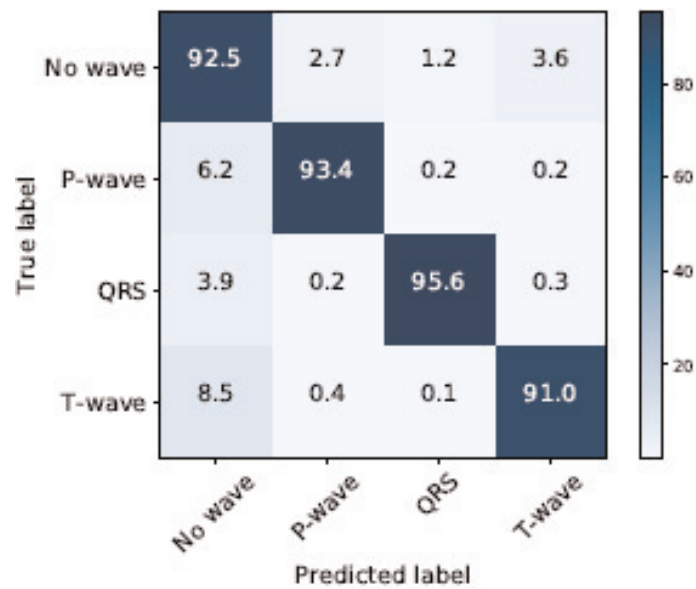
In **Figure 8**, the Conv, BN, and dense imply the convolution, batch normalization, and the fully connected layers whereas the ReLU and σ represents the activation layers namely the rectified linear unit and the sigmoid, respectively. The ResBlk is nothing but the residual block where the internal architecture of each such block is shown in a detailed fashion below the main architecture. In the residual block, the dropout layer represents the dropout regularization.

6. Discussion on the experimental results based on the current state-of-the-art techniques

Figure 9a and **b** demonstrate the DENS-ECG model's confusion matrices for the 5-fold CV and test set, respectively. The no wave class has the majority of incorrect cases in all three classes which are P-wave, QRS, and T-wave or it can be said that the model does not make significant errors in classifying the three major classes (P-wave, QRS, and T-wave). The minimal discrepancy between the 5-fold CV and test outcomes indicates that the model has been effectively trained and does not have an overfitting problem.



(a)



(b)

Figure 9. Confusion matrix [33]. (a) 5-fold Cross Validation. (b) Test set.

As demonstrated in **Figure 10** the performance plot, the DENS-ECG model performs similarly to other models in QRS detection with 99.61% of sensitivity and 99.52% of precision. The wavelet-based model proposed by Martinez et al. has the best performance in terms of sensitivity and accuracy of 99.8 and 99.86%, respectively followed by Kim and Shin's proposed model. The postulated DENS-ECG model performed similarly to the well-known Pan and Tompkins's QRS detection model but it outperformed the QRS detection methods proposed by Poll et al.

In [35], the classification ECG signals from heartbeat were classified into both 7 and 5 arrhythmia classes, respectively. For 5-classification problems, the heartbeats are divided into five categories by the Association for Advancement of Medical Instrumentation (AAMI). normal (N), supraventricular (S) ectopic, ventricular (V) ectopic, fusion (F), and unknown (Q) beats are the four types of an ectopic heartbeat.

Performance Plot

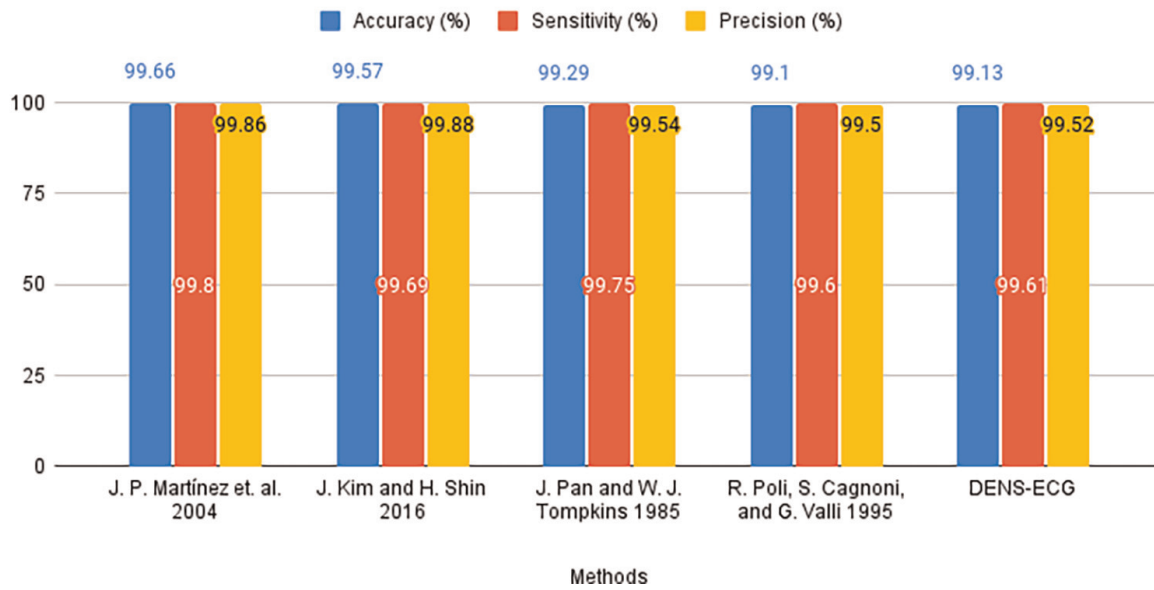


Figure 10. Comparison of DENS-ECG and various deep model architectures' classification performance on the test set [33].

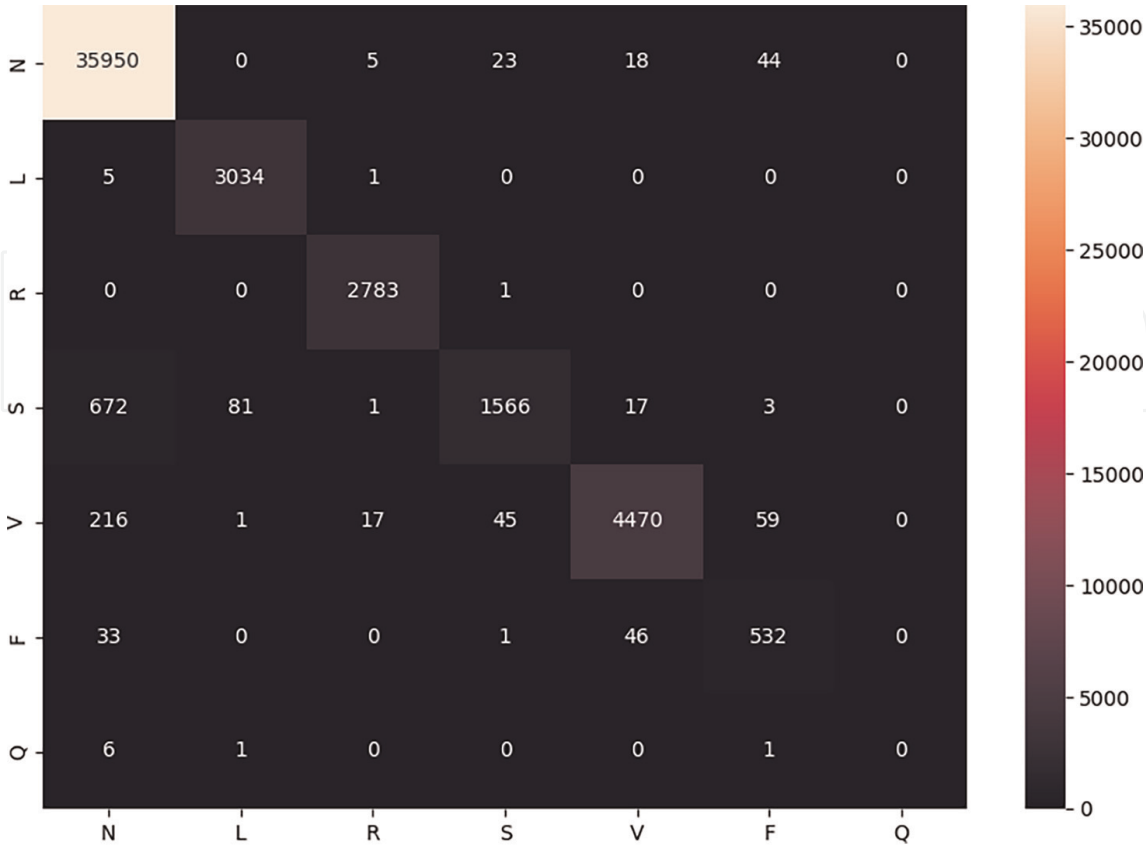
Further, the class N is divided into three more classes in the 7-classification to improve resolution by isolating the two conduction anomalies known as left bundle branch block (L) and right bundle branch block (R). **Figure 11** represent the confusion matrix of 7 and 5-class classification problem, respectively where the former model is capable of effectively distinguishing L and R from N.

As shown in **Figure 12**, Ribeiro et al. [36] has compared DNN's performance indexes to the average performance of 4th-year cardiology residents, 3rd-year emergency residents, and 5th-year medical students. The performance of the DNN on the test set is demonstrated in the above accuracy plot. The above-shown figure shows that the performance of DNN which exceeds human performance. In most cases, the accuracy of DNN on the data set is more than 95%.

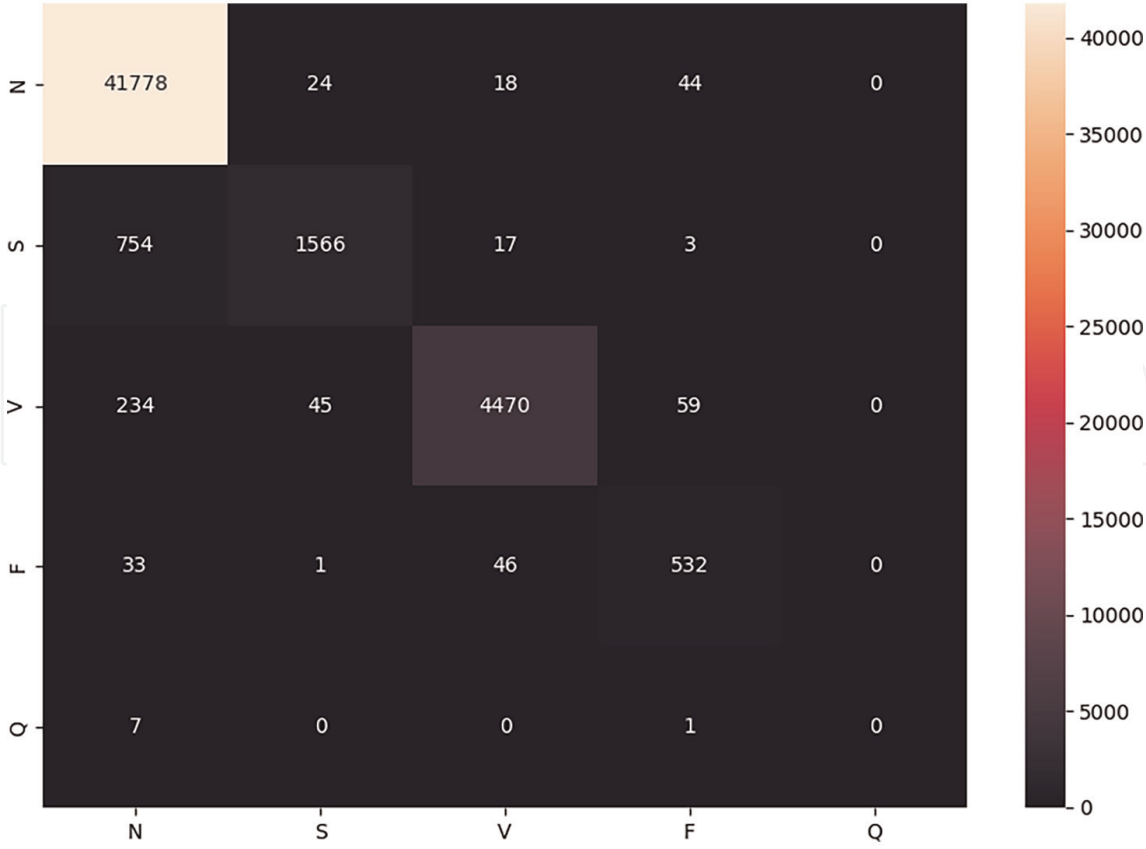
Finally, the work of Jambukia et al. [34] presents a survey on the performance of various works present in the literature which are based on ECG signal categorization utilizing different pre-processing approaches, feature extraction techniques, and classifiers. **Figure 13** presents the plot of the accuracy of different ECG classification techniques which have used the MIT-BIH arrhythmia database over time.

7. Conclusions

Health issues in the human race are increasing day by day and cardiac issues are one of the most common diseases which has been noticed in the past few decades. Therefore, many technologies have been introduced and CAD is the most emerging technology to diagnose cardiac issues or solve heart-related diseases. Furthermore, deep learning has played an important role in the area of computer-aided diagnosis (CAD). From the above discussion, it can be observed that various algorithms or methods have performed pretty well in the field of cardiovascular disease detection. This indicates that deep learning in cardiac signal processing has an unbounded scope in the research field for enhancing CAD and getting more accurate and cost-effective and fast output.



(a)



(b)

Figure 11. Confusion matrix [35]. (a) 7 heartbeat classes. (b) 5 heartbeat classes.

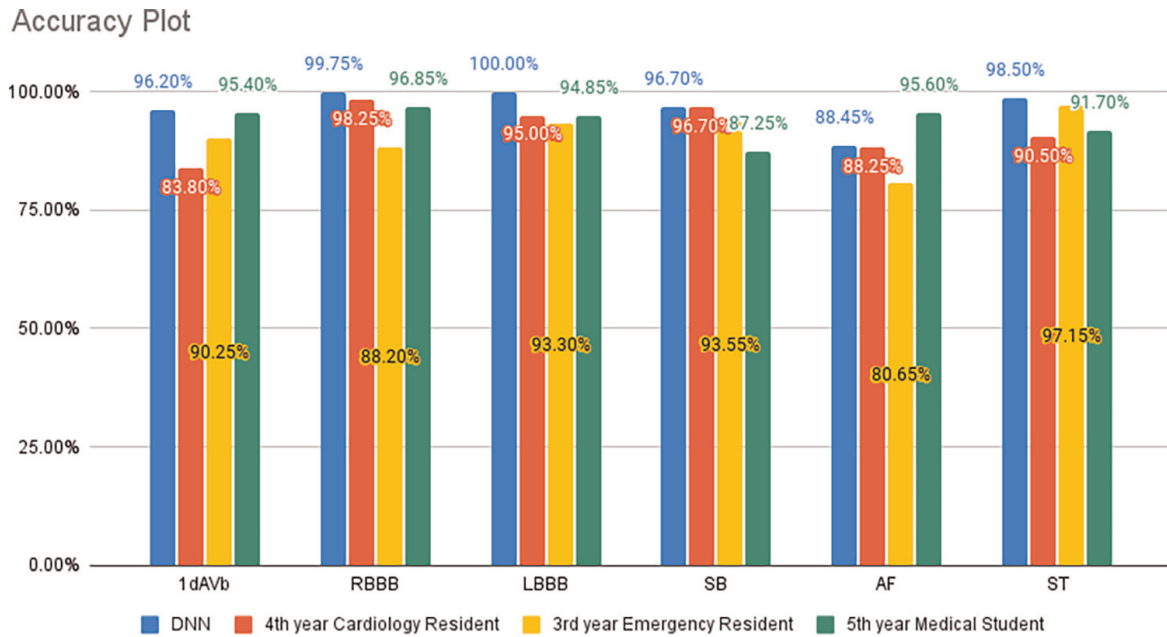


Figure 12. Comparison of performance indexes of DNN and the average performance of cardiology students on the test set [36].

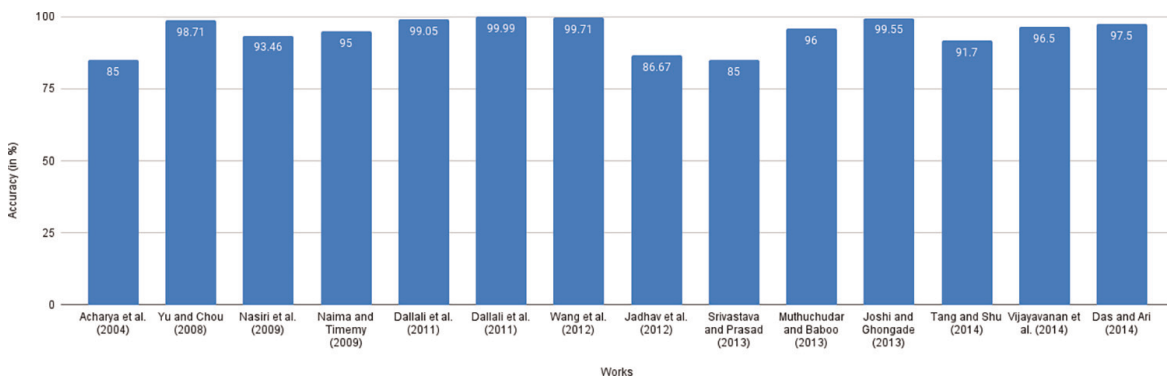


Figure 13. Comparison of the accuracy of the different ECG classification techniques [34].

Conflict of interest

The authors declare no conflict of interest or delete this entire section.

Abbreviations

- ECG electrocardiogram
- CVD cardiovascular disease
- AI artificial intelligence
- ICD International Classification of Diseases
- CAD computer-aided design
- CT computed tomography
- CHF congestive heart failure
- ANN artificial neural network
- CNN convolutional neural network

RNN	recurrent neural network
LSTM	long short-term memory
BI-LSTM	bi-directional long short-term memory
DNN	deep neural networks

IntechOpen

Author details

Sumagna Dey^{1*†}, Rohan Pal^{2†} and Saptarshi Biswas^{3†}

1 Meghnad Saha Institute of Technology, Kolkata, India


2 Kalyani Government Engineering College, Kalyani, India

3 Iowa State University, Ames, USA

*Address all correspondence to: sumagna.dey@gmail.com

† These authors have contributed equally to this work.

IntechOpen

© 2022 The Author(s). Licensee IntechOpen. This chapter is distributed under the terms of the Creative Commons Attribution License (<http://creativecommons.org/licenses/by/3.0>), which permits unrestricted use, distribution, and reproduction in any medium, provided the original work is properly cited. 

References

- [1] Huffman MD, Prabhakaran D, Osmond C, Fall CHD, Tandon N, Lakshmy R, et al. Incidence of cardiovascular risk factors in an Indian urban cohort results from the New Delhi birth cohort. *Journal of the American College of Cardiology*. 2011;57(17): 1765-1774. DOI: 10.1016/j.jacc.2010.09.083
- [2] By 2030, Deaths Due to Heart Disease Likely to Increase by 2.3cr: Doctor. Available from: <https://www.dnaindia.com/jaipur/report-by-2030-deaths-due-to-heart-disease-likely-to-increase-by-23cr-doctor-2667520> [Accessed: 18 December 2021]
- [3] Cardiovascular Diseases (CVDs). Available from: [https://www.who.int/news-room/fact-sheets/detail/cardiovascular-diseases-\(cvds\)](https://www.who.int/news-room/fact-sheets/detail/cardiovascular-diseases-(cvds)) [Accessed: 15 December 2021]
- [4] Olvera Lopez E, Ballard BD, Jan A. Cardiovascular disease. In: *StatPearls*. Treasure Island, FL: StatPearls Publishing; 2022
- [5] Jordaens L. A clinical approach to arrhythmias revisited in 2018: From ECG over noninvasive and invasive electrophysiology to advanced imaging. *Netherlands Heart Journal: Monthly Journal of the Netherlands Society of Cardiology and the Netherlands Heart Foundation*. 2018;26(4):182-189. DOI: 10.1007/s12471-018-1089-1
- [6] Maganti K, Rigolin VH, Sarano ME, Bonow RO. Valvular heart disease: Diagnosis and management. *Mayo Clinic Proceedings*. 2010;85(5):483-500. DOI: 10.4065/mcp.2009.0706
- [7] Saleh M, Ambrose JA. Understanding myocardial infarction [version 1; peer review: 2 approved]. *F1000Research*. 2018;7:1378. DOI: 10.12688/f1000.research.15096.1
- [8] Seetharam K, Brito D, Farjo PD, Sengupta PP. The role of artificial intelligence in cardiovascular imaging: State of the art review. *Frontiers in Cardiovascular Medicine*. 2020;7: 618849. DOI: 10.3389/fcvm.2020.618849
- [9] Sherly SI, Mathivanan G. ECG signal noises versus filters for signal quality improvement. In: *2021 International Conference on Advances in Electrical, Computing, Communication and Sustainable Technologies (ICAECT)*. Piscataway, New Jersey, United States: IEEE; 2021. pp. 1-5. DOI: 10.1109/ICAECT49130.2021.9392621
- [10] Bayoumy K, Gaber M, Elshafeey A, Mhaimed O, Dineen EH, Marvel FA, et al. Smart wearable devices in cardiovascular care: where we are and how to move forward. *Nature Reviews Cardiology*. 2021;18:581-599. DOI: 10.1038/s41569-021-00522-7
- [11] Yanase J, Triantaphyllou E. A systematic survey of computer-aided diagnosis in medicine: Past and present developments. *Expert Systems with Applications*. 2019;138:112821. DOI: 10.1016/j.eswa.2019.112821
- [12] Karssemeijer N. Computer aided detection in breast imaging: More than perception aid. In: *2010 IEEE International Symposium on Biomedical Imaging: From Nano to Macro*. Piscataway, New Jersey, United States: IEEE; 2010. pp. 273-273. DOI: 10.1109/ISBI.2010.5490360
- [13] Wang EK, Zhang X, Pan L. Automatic classification of CAD ECG signals with SDAE and bidirectional long short-term network. *IEEE Access*. 2019;

7:182873-182880. DOI: 10.1109/
ACCESS.2019.2936525

Arrhythmia. 2020;**36**(6):1107.
DOI: 10.1002/joa3.12441

[14] Doi K. Computer-aided diagnosis in medical imaging: Historical review, current status and future potential. *Computerized Medical Imaging and Graphics: The Official Journal of the Computerized Medical Imaging Society*. 2007;**31**(4-5):198-211. DOI: 10.1016/j.compmedimag.2007.02.002

[21] Demystifying the 12 Lead ECG! Available from: <https://nurseyourownway.com/2016/04/20/demystifying-the-12-lead-ecg/> [Accessed: 28 December 2021]

[15] Dey S, Nath P, Biswas S, Nath S, Ganguly A. Malaria detection through digital microscopic imaging using deep greedy network with transfer learning. *Journal of Medical Imaging*. 2021;**8**(5): 054502. DOI: 10.1117/1.JMI.8.5.054502

[22] Al-Qazzaz NK. Comparison of the RLS and LMS algorithms to remove power line interference noise from ECG signal. *Al-Khwarizmi Engineering Journal*. 2021;**6**(2):51-61

[16] Saad NM, Abdullah AR, Low YF. Detection of heart blocks in ECG signals by spectrum and time-frequency analysis. In: 2006 4th Student Conference on Research and Development. Piscataway, New Jersey, United States: IEEE; 2006. pp. 61-65. DOI: 10.1109/SCORED.2006.4339309

[23] Ozyilmaz L, Yildirim T. Artificial neural networks for diagnosis of hepatitis disease. *Proceedings of the International Joint Conference on Neural Networks*. 2003;**1**:586-589. DOI: 10.1109/IJCNN.2003.1223422

[17] *Signal Processing: A Mathematical Approach, Second Edition*. Available from: <https://library.oapen.org/bitstream/id/3eb04f39-67d7-4b4d-8569-3185fbefd944/1005624.pdf> [Accessed: 20 December 2021]

[24] Mao WB, Lyu JY, Vaishnani DK, Lyu YM, Gong W, Xue XL, et al. Application of artificial neural networks in detection and diagnosis of gastrointestinal and liver tumors. *World Journal of Clinical Cases (WJCC)*. 2020; **8**(18):3971-3977. DOI: 10.12998/wjcc.v8.i18.3971

[18] *Discrete-Time/Frequency Analysis*. Available from: https://ccrma.stanford.edu/courses/150-2001/time_frequency.html [Accessed: 31 December 2021]

[25] Krizhevsky A, Sutskever I, Hinton GE. ImageNet classification with deep convolutional neural networks. *Communications of the ACM*. 2017; **60**(6):84-90. DOI: 10.1145/3065386

[19] Sampling Theorem. Available from: <https://www.sciencedirect.com/topics/engineering/sampling-theorem> [Accessed: 28 December 2021]

[26] Takase H, Gouhara K, Uchikawa Y. Time sequential pattern transformation and attractors of recurrent neural networks. In: *Proceedings of 1993 International Conference on Neural Networks (IJCNN-93-Nagoya, Japan)*. Vol. 3. Piscataway, New Jersey, United States: IEEE; 1993. pp. 2319-2322. DOI: 10.1109/IJCNN.1993.714189

[20] Yoneyama K, Naka M, Harada T, Akashi Y. Creating 12-lead electrocardiogram waveforms using a three-lead bedside monitor to ensure appropriate monitoring. *Journal of*

[27] Sunny MAI, Maswood MMS, Alharbi AG. Deep learning-based stock price prediction using LSTM and bi-

directional LSTM model. In: 2020 2nd Novel Intelligent and Leading Emerging Sciences Conference (NILES). Piscataway, New Jersey, United States: IEEE; 2020. pp. 87-92. DOI: 10.1109/NILES50944.2020.9257950

[28] LSTM and Its Equations. Available from: <https://medium.com/@divyanshu132/lstm-and-its-equations-5ee9246d04af> [Accessed: 2 January 2022]

[29] Yu X, He J, Zhang Z. Facial image completion using bi-directional pixel LSTM. *IEEE Access*. 2020;**8**: 48642-48651. DOI: 10.1109/ACCESS.2020.2975827

[30] Xiang J, Qiu Z, Hao Q, Cao H. Multi-time scale wind speed prediction based on WT-bi-LSTM. *MATEC Web Conference*. 2020;**309**:05011. DOI: 10.1051/mateconf/202030905011

[31] Dey S, Biswas S, Nandi S, Nath S, Das I. Deep greedy network: A tool for medical diagnosis on exiguous dataset of COVID-19. In: 2020 IEEE 1st International Conference for Convergence in Engineering (ICCE). Piscataway, New Jersey, United States: IEEE; 2020. pp. 340-344. DOI: 10.1109/ICCE50343.2020.9290715

[32] Subashini A, Raghuraman G, Sai Ramesh L. Enhancing the classification accuracy of cardiac diseases using image denoising technique from ECG signal. In: 2019 International Conference on Computational Intelligence in Data Science (ICCIDS). Piscataway, New Jersey, United States: IEEE; 2019. pp. 1-4. DOI: 10.1109/ICCIDS.2019.8862168

[33] Peimankar A, Puthusserypady S. DENS-ECG: A deep learning approach for ECG signal delineation. *Expert Systems with Applications*. 2020;**165**: 113911

[34] Jambukia SH, Dabhi VK, Prajapati HB. Classification of ECG signals using machine learning techniques: A survey. In: 2015 International Conference on Advances in Computer Engineering and Applications. Piscataway, New Jersey, United States: IEEE; 2015. pp. 714-721. DOI: 10.1109/ICACEA.2015.7164783

[35] Saadatnejad S, Oveisi M, Hashemi M. LSTM-based ECG classification for continuous monitoring on personal wearable devices. *IEEE Journal of Biomedical and Health Informatics*. 2020;**24**(2):515-523. DOI: 10.1109/JBHI.2019.2911367

[36] Ribeiro AH, Ribeiro MH, Paixão GMM, Oliveira DM, Gomes PR, Canazart JA, et al. Automatic diagnosis of the 12-lead ECG using a deep neural network. *Nature Communications*. 2020;**11**(1):1760. DOI: 10.1038/s41467-020-15432-4